jet INTL JOURNAL OF ELECTRONICS AND TELECOMMUNICATIONS, 2022, VOL. 68, NO. 1, PP. 91-96
Manuscript received August 29, 2021; revised January, 2022. DOI: 10.24425/ijet.2022.139853

Generation of Large-area Arrays of Aperiodic Functional Micro/nano Structures Using Phase Shift Interferometry

Pearly Princess. J[1], A. Alfred Kirubaraj[1], S. Christina Sophia[1], S. Senith[1], S.R. Jino Ramson[2]

***Abstract*—Phase shift interferometry (PSI) derived from interference technique as greater surface characterization technique based on the interference information recorded during a controlled phase shift. This research shows the development of micro/nano structures using phase shift interferometry. (PSI) is the process of developing the complex pattern structure using variable phase angle between two or more beams aligned to obtain functional aperiodic arrays. We have designed and modelled the PSI and simulated through MATLAB in 2D and 3D pattern structures. The PSI was performed in two process analysis. First, without PSI referring normal interference technique. Second, with PSI referring position of laser beams in quadrant-based alignment. The obtained results show the minimum feature structure was measured as 12 nm. This feature size developed under phase shift interferometry (PSI) produces minimum feature size compared to the existing interferometry technique. This study gives the promising increased fabrication area could develop large area arrays structures.**

***Keywords*—laser interference lithography (LIL); pattern structures; periodic and aperiodic pattern; phase shift interferometry (PSI)**

I. Introduction

PERIODICALLY patterned surfaces not only have unique characteristics, but also serve as intelligent surfaces that can selectively affect various functionalities in biomaterials, surface engineering, photonics and sensor systems applications [1-5]. Several methods for designing and producing such micro- and nano-functions have been studied and applied (e.g. lithographic nano-printing, laser writing, and optical lithography). However, in a single process step only a few of these are suitable for the manufacture of periodic structures on different materials. One of the more recent developments in surface texture within the micro- and sub-micrometer scale [8] is phase-shift interferometry. The design of patterned structures and miniaturization in size play a vital role in their realization and fabrication in this technique. The method provides an excellent opportunity to build structures on both planar and non-planar surfaces with minimal feature size less than 20 nm. Unlike other methods, PSI greatly enhances large-area output (up to several cm2/s) using single or multiple laser pulses, unlike other surface patterning methods. Consequently, it provides an efficient route to large-scale development. The detailed explanation is derived and modelled mathematically. The intensity distribution of the interfering laser beams can be defined as below for a multi-beam interference pattern [12-14]:

$$I = \frac{c\varepsilon_0}{2}\left|\sum_{j=1}^{n} E_j\right|^2 \quad (1)$$

Where E_j is the main component of the light wave field, the speed of light is c, and vacuum permittivity is ε_0. The intensity measurement is very important for phase shifting interferometry. (1). Since the laser beams has the wavelength the spatial period also needed to be calculated which is the distance between the consecutive corresponding points of same phase on the wave (2). A similar line such as periodic distribution is obtained in the case of a pattern of two-beam interference and its spatial length (both) is indicated by [15]:

$$\Lambda = \frac{I}{2\sin\left(\frac{\alpha}{2}\right)} \quad (2)$$

Where λ is the laser's wavelength and λ is the angle between the two lasers. Consequently, for a given wavelength with a resolution down to half the wavelength (λ/2), which corresponds to an angle (a) of 180 between the interfering beams, the periodic modulation of the interference pattern can be controlled. PSI is concerned with the use of interference patterns generated from two or more coherent laser radiation beams as a tool for structuring materials. In this research paper, Section. 2 describe the alignment of four-beams, Section 3 deals with PSI mathematical modeling. In section 4. the experimental outcomes and their discussions are discussed. Section 5 is about conclusion.

II. Phase-Shift Interferometry

The interference patterns may be laser beam lines or dot arrays or matrices. The intensity distribution of the interference patterns shows structures with a sub-wavelength light pitch that intervenes. It is possible to grow feature sizes down to a fraction of the laser wavelength by using such radiation to interact with materials. Fig. 1 exhibits the scheme of a phase shift interferometry system. This technology provides a way for nano patterns to be periodic and quasi-periodic patterns, which are spatially consistent across large areas.

Pearly princess. J[1], A. Alfred Kirubaraj[1]*, S. Christina Sophia[1], S. Senith[1] are with Karunya Institute of Technology and Sciences, Karunya Nagar, India (e-mail: alfred@karunya.edu).
S.R. Jino Ramson[2] is with VIT Bhopal University, Bhopal, India.

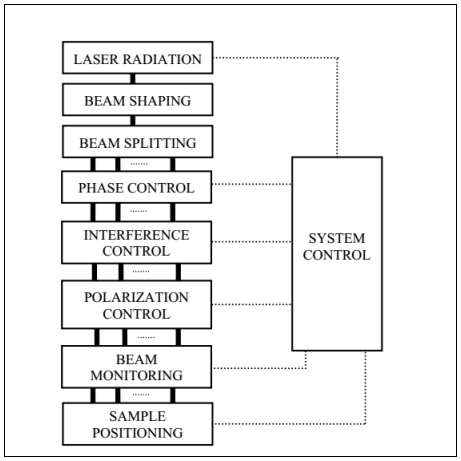

Fig. 1. Scheme of a phase-shift interferometry system

PSI is highly advanced in nanolithography because of its high efficiency, large work areas and low cost of structuring nano-scale material compared to ion beam lithography (IBL) or electron beam lithography technology (EBL). The benefit of LIL in terms of scanning probe lithography (SPL) technology is the non-contact projection mode with a long working distance and intense operation. Because we are based on several beams, light wave superposition occurs as the core concept in phase shifting. The general form of N-beam interference can be described as the overlapping of electric field vectors of N laser beams. (E_1, E_2, E_3, ..., EN). Its formulation can be represented as (3)

$$\vec{E} = \sum_{m=1}^{N} \vec{E}_m = \sum_{m=1}^{N} A_m \vec{p}_m \cos(kn_m.r_m \pm 2\pi vt + \phi_m) \quad (3)$$

Where Am (m = l, 2, ..., N) is the amplitude, pm (m = l,2, ..., N) is the unit polarization vector, k=2πγ is the number of waves, nm (m = l, 2, ..., N) is the unit vector in the direction of propagation, rm is the vector of position, v is the frequency and φm (m = l, 2, ..., N) is the phase constant. When N is allocated to 4 the patterns of interference can be dot arrays. **Fig. 2** exhibits the 4-beam laser interference theory [3].

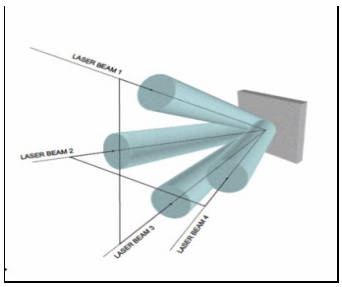

Fig. 2. Intensity distribution of multi-beam alignment

There are three criteria for interacting with the laser beams. First, the same intensity (A_o) should apply to four beams. Second, Laser beam 1 and laser beam 3 shall be in the same plane and at the same angle of incident to the sample plane. This principle applies to the other two beams, as well. Third, the plane in which the laser beams1 and 2 are in must be perpendicular to the plane in which the other two beams are in. On beam incidence with symmetrical incidence angle, the distribution of intensity is derived as:

$$I = 2\times(A_0)^2\{(2+\cos(2kx\sin\theta)+\cos(2ky\sin\theta)+2\cos(k(x-y)\sin\theta)+2\cos(k(x+y)\sin\theta))\} \quad (4)$$

III. Modelling of PSI

A light source is positioned at the point 'p' distance of the slit's separation is 'd', and some distance away a projection screen is placed from sources S_1, S_2 and S_3. Assuming that the distance is much greater than the distance between the two slits from the source to the screen i.e., L>>d shown in **Fig. 3** In order to achieve maximum interference on the screen, the first path difference is $\Delta r_1 = d\sin\theta$ and second difference is $\Delta r_2 = 2d\sin\theta$ and phase difference is given by first phase difference $\Delta\phi_1 = 2\pi\frac{d\sin\theta}{\lambda}$, and second phase difference, $\Delta\phi_2 = 2\pi\frac{2d\sin\theta}{\lambda}$.

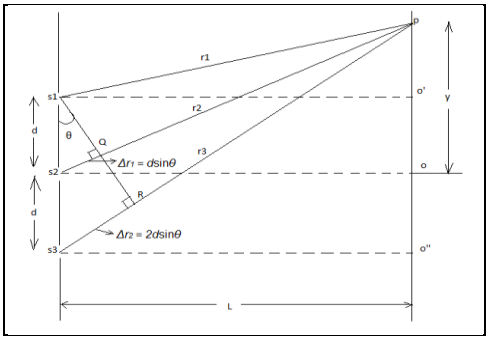

Fig. 3. Three beam phase shift interferometry alignment

By using above diagram, the separation of slits will be able to see clearly from source to screen. The three-beam interference which consist three slits. The distance of the slits are 'd' and length from source to screen is 'L', the three sources meeting at the point 'P' at distance from 'O' to 'P' is 'Y'. Let the three waves from the slits are Suppose source of light passes through three slits, each separated by a distance d from its neighbor.

$$E_1 = E_0\sin(\omega t) \quad (5)$$

$$E_2 = E_0\sin(\omega t+\phi) \quad (6)$$

$$E_3 = E_0\sin(\omega t+2\phi) \quad (7)$$

$$\sin a+\sin b = 2\cos(\frac{a-b}{2})\sin(\frac{a+b}{2}) \quad (8)$$

Adding the equation (5) and (7)

$$E_1+E_3 = E_0\sin(\omega t)+E_0\sin(\omega t+2\phi) \quad (9)$$

$$E_1 + E_3 = E_0[\sin(\omega t) + \sin(\omega t + 2\phi)] \quad (10)$$

$$E_1 + E_3 = 2E_0 \cos\phi \sin(\omega t + \phi) \quad (11)$$

$$E = 2E_0 \cos\phi \sin(\omega t + \phi) + E_0 \sin(\omega t + \phi) \quad (12)$$

$$E = E_0(1 + 2\cos\phi)\sin(\omega t + \phi) \quad (13)$$

Hence from the equation (14) it is theoretically derived and the intensity calculation for multiple beams supports the principle of phase-shift interference.

IV. Results and Discussion

Phase-shift interferometry (PSI) produces the promising results on tunability factors over the lithographic interference system. It is observed that the mathematical modelling of PSI records the intensity factor depends on and beam phase angle that produces different asymmetric structures on MATLAB simulation. Also, the dependent factors include slit separation (d), length from source to screen (L) and wavelength of each beam (λ). We have simulated the PSI in different parameter studies in varying slit separation (d), length (L), wavelength (λ) and phase angle of each beam (φ). we have simulated and generated the phase shift interference through MATALAB and obtained 2D, 3D and 2D-FFT patterned structures for the wavelength (λ) as 750 nm, varying slit separation (d) as 0.0125 µm and 0.0225 µm, length as from source to screen (L) as 2 mm. The generated patterned structures compare both with PSI and without PSI. The comparison study shows, the varying slit separation gives the promising result over the generated periodicity. For the slit separation 0.0125 µm produces the periodicity value for without PSI as 0.148 µm and with PSI producing 0.013 µm. In the same way on increasing the slit separation to 0.0225 µm produces the periodicity for without PSI as 0.11 µm and with PSI producing 0.012 µm. Hence the interferometry of the phase shift rules over the focal length on varying slit separation and controls over the periodicity of the beams. Fig. 4-11 concludes lesser the slit separation between the beams produces the minimum periodicity range and produces various pattern structures with shapes in 2D-FFT. The simulation results show with and without PSI affecting the nature of interference and having linear line shapes with intensity distribution across the beam.

Pattern generation for phase shifting interference for wavelength (λ) = 750 nm, slit separation (d) =0.0125 µm, length (l) = 2 mm (with and without PSI)

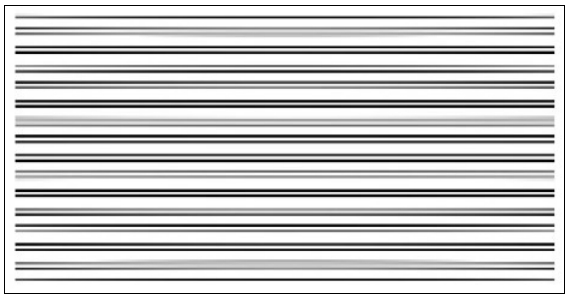

Fig. 4. 2D pattern generation- Without PSI

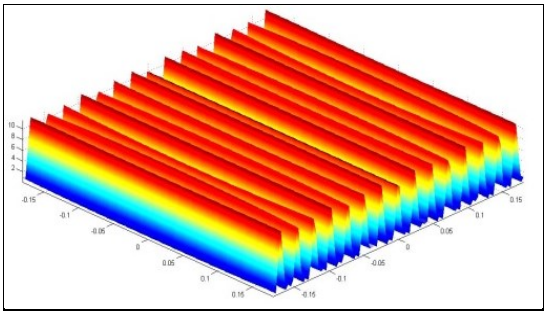

Fig. 5. 3D pattern generation- Without PSI

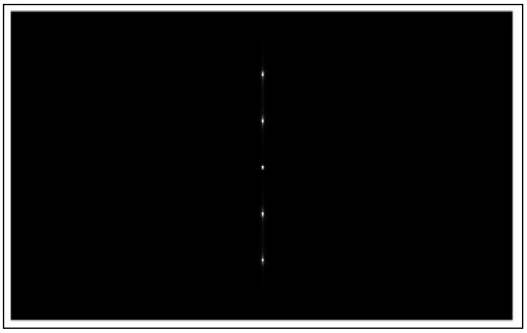

Fig. 6. 2D FFT generation- Without PSI

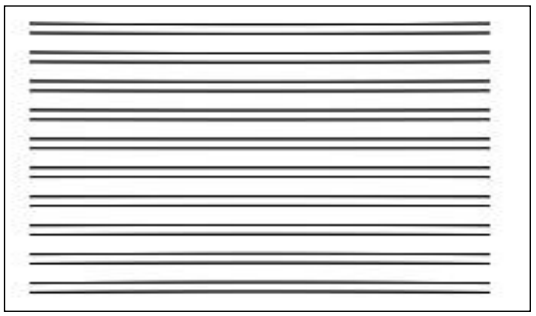

Fig.7. 2D pattern generation- With PSI

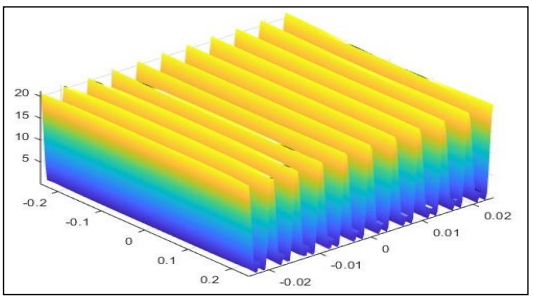

Fig. 8. 3D pattern generation- With PSI

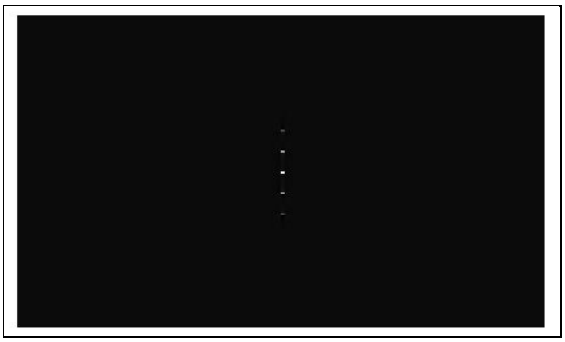

Fig. 9. 2D FFT generation- With PSI

TABLE I
VARIATION IN PERIODICITY FOR DIFFERENT WAVELENGTH

Wavelength (nm)	Periodicity (μm)
550	0.11
650	0.13
750	0.15
850	0.16
950	0.17
1050	0.18

Table I plots on varying wavelength producing periodicity pattern in nm range. Thus, it shows the relation between wavelength and generated periodicity. The simulated laser beam with varying wavelength from 550 nm ~1050 nm was performed and corresponding periodicity for with PSI was calculated. The calculated value resumes the prominent results showing as the wavelength of the beam decreases the periodicity value also decreases. Hence the tabulation shows wavelength of the beam is directly proportional to the generated periodicity. Varying the wavelength also leads to the formation of complex pattern structures and increased depth of focus. We could see the linear rise between wavelength and periodicity concludes as wavelength increases the periodicity increases and vice versa is shown in Fig. 10**.**

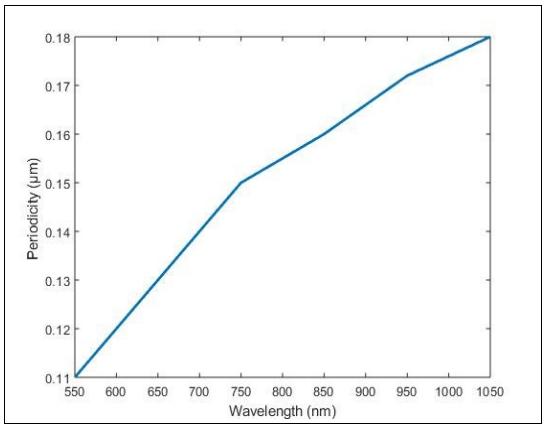

Fig. 10. Variation in periodicity for different wavelength

Further parametric analyses are carried out to study the factor affecting the interference on phase-shift. Variation in periodicity for different slit separation between the beams was studied. The simulated laser beam with varying slit separation distance from 1.25 mm ~75 mm was performed and corresponding periodicity for with PSI was calculated. The calculated value resumes the prominent results showing as the slit separation from source to beam decreases the periodicity value also decreases. Hence the tabulation shows slit separation from source to beam is directly proportional to the generated periodicity. Varying the slit separation also leads to the formation of complex pattern structures and the shape function is shown in Table II and Fig. 11

The variation in periodicity for different length to perform symmetry phase shift interference. The simulated laser beam with varying length from 4 mm – 200 mm was performed and corresponding periodicity for with PSI was calculated. The calculated value resumes the prominent results showing as the length of the beam from point to screen decreases the periodicity value also decreases. Hence the tabulation shows length of the beam is directly proportional to the generated periodicity. Dynamic positioning of the laser beam and tuning the length leads to generation of micro/Nano structures on large area.

Table II
VARIATION IN PERIODICITY FOR DIFFERENT SLIT SEPARATION

Slit separation (mm)	Periodicity (μm)
1.25	2.1
20	5
35	8
50	10
75	20

TABLE III
VARIATION IN PERIODICITY FOR DIFFERENT LENGTH

HD	VD=0
4	0.33
10	0.356
25	0.63
120	0.77
200	2.07

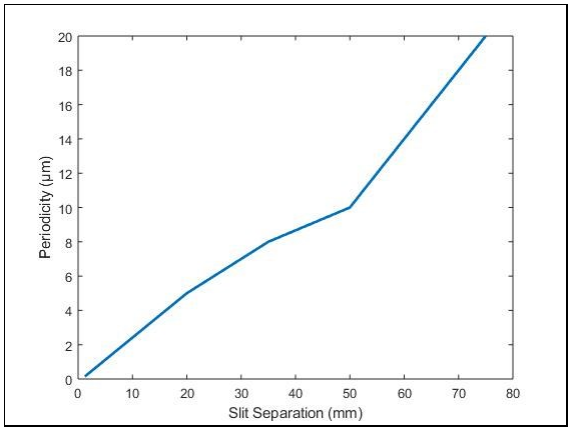

Fig. 11. Variation in periodicity for varying slit separation

CONCLUSION

The phase shift interferometry technique can be an alternative solution to the normal interference technique (PSI). The interference technique uses intersection angle between the beams but in phase shift interferometry technique uses angles for each individual beam to control over the topology of the pattern structures.

From Table IV, it is clear that the referenced papers have designed and simulated patterns with wavelength that ranges between 10 nm-1064 nm and obtained a periodicity of about 20 nm-10 μm. But they failed to focus on the size optimization. In the research paper by Adrien Chauvin, he has reported the periodicity of 1μm for a wavelength of 350 nm.

TABLE IV
COMPARISON OF DIFFERENT REFERENCE PAPER'S RESULTS

Authors	Wavelength (nm)	Periodicity (nm)
Andreas Winter	300	500
Adrien Chauvin	350	1µ
Swagato Sarkar	405	15
Shuzo Masui	450	140
Jun Wu Orc I	500	273
Seyedeh Mahsa Kamali	532	482
Chiara Valsecchi	1064	575, 675
Min Jin Kang	1064	1µ
***Our Research Paper**	**750**	**12**

The author Min Jin Kang has reported the periodicity of about 1µm for a wavelength of 1064 nm. But whereas we could attain the periodicity of about 18 nm for a wavelength of 1050 nm. The author Chiara Valsecchi has reported the periodicity of about 575 nm and 675 nm for a wavelength of 1064 nm. But whereas we could attain the periodicity of about 18 nm for a wavelength of 1050 nm. The author Seyedeh Mahsa Kamali, has reported the periodicity of about 482 nm for a wavelength of 532 nm. But whereas we could attain the periodicity of about 11 nm for a wavelength of 550 nm. The author Andreas Winter has reported the periodicity of about 500 nm for a wavelength of 300 nm. The author Swagato Sarkar, has reported the periodicity of about 15 nm for a wavelength of 405 nm. But whereas we could attain the periodicity of about 11 nm for a wavelength of 550 nm. The author Shuzo Masui, has reported the periodicity of about 140 nm for a wavelength of 450 nm. But whereas we could attain the periodicity of about 11 nm for a wavelength of 550 nm. The author Jun Wu Orc I has reported the periodicity of about 273 nm for a wavelength of 500 nm. But whereas we could attain the periodicity of about 11 nm for a wavelength of 550 nm as shown in Fig.12.We have designed the PSI and performed minimal feature size to generate micro/nano patterns structures and obtained a periodicity of about 12 nm with the slit separation between the beams as 0.0225 µm with the applied wavelength of 750 nm is shown in Fig. 13. Hence the phase shift interferometry concludes that PSI can produce minimal periodicity feature size than normal interference technique. From the above depicted results, the use of micro/nano structure through PSI can be widely used in silicon surface, micro patterning, nanowire manufacturing, Nano-ribbon, hole arrays, anti-reflection film-based hybrid-polymer nanostructures and 2D/3D photonic structures, graphene oxide-based humidity sensing system and hybrid plasmonic structure.

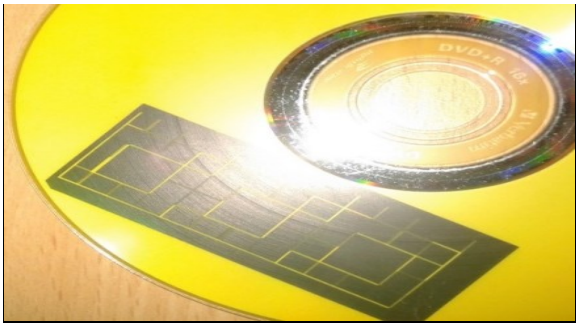

Fig.12. Periodicity of about 11 nm for a wavelength of 550 nm-Light scribe Technology

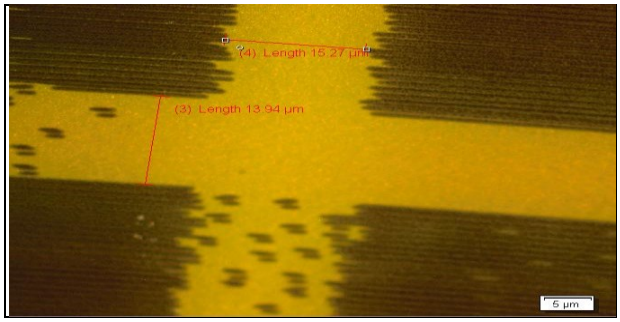

Fig. 13. Periodicity of about 12 nm for a wavelength of 750 nm-Light scribe Technology.

ACKNOWLEDGEMENTS

We are very grateful to Karunya Institute of Technology and Sciences for providing the lab facility to carry out the research in Laser Interference Lithography Lab Facility to generate and analyze the pattern generated from LIL Lab.

REFERENCES

[1]. AAsenbaum, P., Overstreet, C., Kovachy, T., Brown, D. D., Hogan, J. M., &Kasevich, M. A. (2017). *Phase Shift in an Atom Interferometer due to Spacetime Curvature across its Wave Function.* Physical Review Letters, 118(18), 1–5. https://doi.org/10.1103/PhysRevLett.118.183602.

[2]. Adela Habib, RensselaerHarikrishnanVijayamohanan, Chaitanya K. Ullal, and RavishankarSundararaman. (2020). *Coupled Electromagnetic and Reaction Kinetics Simulation of Super-WResolution Interference Lithography*. J. Phys. Chem. B 2020, 124, 35, 7717–7724. https://doi.org/10.1021/acs.jpcb.0c05194

[3]. Adrien Chauvin et al. (2017). *Large scale fabrication of porous gold nano wires via laser interference lithography and dealloying of Gold-Silver-Nano-alloys*. Micromachines 2017, 8(6),168. https://doi.org/10.3390/mi8060168 .

[4]. AndreasWinter1, YasinEkinci, Armin Gölzhäuser and Andrey Turchanin (2019). *Freestanding carbon nano-membranes and graphene monolayers nano-patterned via EUV interference lithography*. IOP Publishing Ltd 2DMaterials, 6(2). https://doi.org/10.1088/20531583/ab0014

[5]. Baek, Y., Lee, K., Yoon, J., Kim, K., & Park, Y. (2016). *White-light quantitative phase imaging unit. Optics Express*, 24(9), 9308. https://doi.org/10.1364/oe.24.009308.

[6]. Chauvin, A., Stephant, N., Du, K., Ding, J., Wathuthanthri, I., Choi, C. H., El Mel, A. A. (2017). *Large-scale fabrication of porous gold nanowires via laser interference lithography and dealloying of gold-silver nano-alloys.* Micromachines,8(6). https://doi.org/10.3390/mi8060168.

[7]. Jywe, W. Y., Wang, M. S., & Wu, C. H. (2016). *Application of blue laser direct-writing equipment for manufacturing of periodic and aperiodic nanostructure patterns*. Precision Engineering, 46, 263–269. https://doi.org/10.1016/j.precisioneng.2016.05.006.

[8]. Chiara Valsecchi *, Luis Enrique Gomez Armas and Jacson Weber de Menezes. (2019). *Large Area Nano-hole Arrays for Sensing Fabricated by Interference Lithography*. Optical Chemical Nano sensors, Sensors 2019, 19(9),2182; https://doi.org/10.3390/s19092182.

[9]. D'Amico, G., Rosi, G., Zhan, S., Cacciapuoti, L., Fattori, M., &Tino, G. M. (2017). *Canceling the Gravity Gradient Phase shift in Atom Interferometry*. Physical Review Letters, 119(25),1–6. https://doi.org/10.1103/PhysRevLett.119.253201.

[10]. Deng, X., Hu, Z., Xiu, G., Song, Z., Weng, Z., Xu, J., Wang, Z. (2010). *Five-beam interference pattern model for laser interference lithography*. 2010 IEEE International Conference

on Information and Automation, ICIA 2010, (Cd), 1208–1213. https://doi.org/10.1109/ICINFA.2010.5512128.

[11]. Di, J., Li, Y., Xie, M., Zhang, J., Ma, C., Xi, T., Zhao, J. (2016). *Dual-wavelength common-path digital holographic microscopy for quantitative phase imaging based on lateral shearing interferometry*. Applied Optics, 55(26), 7287. https://doi.org/10.1364/ao.55.007287

[12]. Guo, L., Jiang, H. B., Shao, R. Q., Zhang, Y. L., Xie, S. Y., Wang, J. N., Sun, H. B. (2012). *Two-beam-laser interference mediated reduction, patterning and nano structuring of graphene oxide for the production of a flexible humidity sensing device*. Carbon, 50(4), 1667–1673. https://doi.org/10.1016/j.carbon.2011.12.011.

[13]. Guo, T., Li, F., Chen, J., Fu, X., & Hu, X. (2016). *Multi-wavelength phase-shifting interferometry for micro-structures measurement based on color image processing in white light interference*. Optics and Lasers in Engineering, 82, 41–47. https://doi.org/10.1016/j.optlaseng.2016.02.003

[14]. Hassan, S., Sale, O., Lowell, D., Hurley, N., & Lin, Y. (2018). *Holographic fabrication and optical property of graded photonic super-crystals with a rectangular unit super-cell*. Photonics, 5(4). https://doi.org/10.3390/photonics5040034

[15]. Hayasaki, Y., Nishitani, M., Takahashi, H., Yamamoto, H., Takita, A., Suzuki, D., & Hasegawa, S. (2012). *Experimental investigation of the closest parallel pulses in holographic femtosecond laser processing*. Applied Physics A: Materials Science and Processing, 107(2), 357–362. https://doi.org/10.1007/s00339-012-6801-1

[16]. Jun Wu OrcID, ZhaoxinGeng, Yiyang Xie Zhiyuan Fan, Yue Su, Chen Xu and Hongda Chen (2019). *The Fabrication of Nanostructures on Polydimethylsiloxane by Laser Interference Lithography*. Nanomaterials 2019, 9(1),73. https://doi.org/10.3390/nano9010073